

Characterisation by TEM and X-ray diffraction of linearly graded composition InGaAs buffer layers on (001) GaAs

F. J. Pacheco, D. Araújo, S. I. Molina, R. García, A. Sacedón, F. González-Sanz, E. Calleja, P. Kidd, and M. A. Lourenço

The dislocation distribution in linearly graded composition layers of InGaAs on GaAs is studied by transmission electron microscopy (TEM). Dislocations are shown to penetrate into the substrate and to invade the first part of the graded layer. A simple balance of forces model predicts the presence of dislocations in the substrate. The observed dislocation distribution in the first region of the graded layer is compared to that predicted by several models. The differences between the models' predictions and observations reported here are discussed. The description of the strain relaxation mechanism given by Dunstan's model is shown to give the best fit to the results reported in the present paper. MST/3444

Dr Pacheco, Dr Araújo, Dr Molina and Dr García are in the Departamento de Ciencia de los Materiales e I.M. y Q.I., Universidad de Cádiz, Cádiz, Spain, Dr Sacedón, Dr González-Sanz, and Dr Calleja are in the Departamento de Ingeniería Electrónica, E.T.S.I. de Telecomunicaciones, Universidad Politécnica de Madrid, Madrid, Spain, and Dr Kidd and Dr Lourenço are in the Department of Materials Science and Engineering, University of Surrey, Guildford, Surrey, UK. This paper was presented at the 1st international conference on Materials for Microelectronics, held in Barcelona, Spain on 17–19 October 1994. © 1998 The Institute of Materials.

Introduction

At present, one of the most important goals of modern semiconductor technology is the fabrication of efficient optoelectronic devices working at waveguide minimum absorption conditions ($\sim 1.5 \mu\text{m}$). Such devices can be provided by III-V semiconductor technology through the use of ternary and quaternary alloys. However, owing to the lattice mismatch with commercial substrates, dislocations are generated which can thread up to the epilayer surface. These threading dislocations degrade considerably the microelectronic and optoelectronic properties of such materials.

The usual approach to avoid the existence of threading dislocations close to the epilayer surfaces in III-V semiconductor heterostructures is to grow a thick relaxed buffer layer between the epilayer and the substrate. To date, most efforts have been oriented to the growth of single constant composition buffer layers and/or superlattice filters. Unfortunately, threading dislocations often propagate through the buffer reaching the active layers. More recently, the possibility of growing relaxed graded composition layers to reduce the threading dislocation densities has been considered. A drastic reduction of such dislocation densities and an almost complete strain relaxation have already been reported for large lattice mismatched systems such as SiGe/Si (Ref. 1), InGaAs/GaAs (Refs. 1–5), or InGaAs/InP (Ref. 6). These results represent an important improvement that confirms this option as a very promising one.

In the present work, the dislocation distribution in linearly-graded composition InGaAs buffer layers grown on GaAs (001) substrates is characterised by transmission electron microscopy (TEM). The TEM observations are compared with the dislocation distribution predicted by several theoretical models.^{7,8}

Experimental technique

The specimens under study were grown by molecular beam epitaxy (MBE) at a growth temperature of 500°C and their layer structures consist of a $1 \mu\text{m}$ thick linearly graded InGaAs (0–28 at.-%In) buffer layer followed by a 250 nm thick InGaAs cap layer (with different In compositions) on a GaAs (001) substrate (Fig. 1).

Conventional TEM studies were performed with a Jeol 1200-EX transmission electron microscope operating at 120 kV. The plan-view TEM (PVTEM) specimen preparation was carried out by chemical etching methods ($\text{Br}_2 + \text{CH}_3\text{OH}$ or $\text{H}_2\text{SO}_4 + \text{H}_2\text{O}_2 + \text{H}_2\text{O}$), and the cross-sectional TEM (XTEM) specimens were prepared by Ar⁺ ion milling after mechanical thinning.

The dislocation Burgers vectors analysis was performed using the two conventional invisibility criteria, $\mathbf{g} \cdot \mathbf{b} = 0$ and $\mathbf{g} \cdot (\mathbf{b} \wedge \mathbf{u}) = 0$, where \mathbf{b} is the Burgers vector of the dislocation, \mathbf{g} is the diffraction vector and \mathbf{u} is the unit vector along the dislocation line direction, for the {220}, {004}, and {111} reflections.

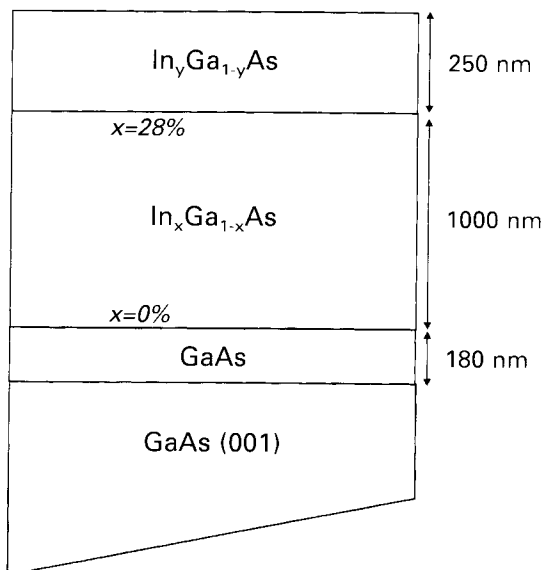
To determine the alloy composition and the strain relaxation of the cap layers, double crystal X-ray diffraction (DCXRD) measurements were carried out. Rocking curves from DCXRD were obtained for each of the specimens from the surface symmetrical (004) and asymmetrical low and high angle (115) reflections using a Bede Scientific Instrument 150 diffractometer. For each specimen, four (004) rocking curves were recorded, where the projection in the (001) plane of the incident and diffracted beams lie along the four $\langle 110 \rangle$ directions. From these four readings any macroscopic tilt between the layer and the substrate was calculated, and was subsequently used to correct peak splitting on the corresponding (115) rocking curves. The standard assumptions have been used to calculate compositions and lattice mismatches.^{9–13}

Experimental results and discussion

A detailed analysis of the plan-view TEM images of the $\sim 250 \text{ nm}$ thick InGaAs cap layers, as shown in Fig. 2, does not reveal the presence of any threading dislocations. Therefore, the dislocation density at the top of the grading and in the cap layers is below the detection limit of this technique, i.e. $< 10^5 \text{ cm}^{-2}$.

Table 1 Results from TEM and XRD obtained for top layers of set of specimens

Specimen	In content, %	Relaxation, %	Top layer thickness, nm
A	15	...	~ 250
B	20.5	94 ± 5	~ 250
C	22.5	88 ± 5	~ 235



1 Schematic description of specimen structures: thicknesses correspond to nominal ones

Plan-view TEM and cross-sectional TEM micrographs (Fig. 2a and b, respectively) reveal the presence of misfit dislocations mainly running along the $[110]$ and $[\bar{1}\bar{1}0]$ directions in the InGaAs buffer layers up to a critical thickness z_c . The measured z_c values are shown in Table 2. The mean cross-sectional density of such defects in the dislocation rich area is $8.7 \pm 1 \times 10^9 \text{ cm}^{-2}$, with a rather uniform distribution. Stereoscopic examination reveals dislocations arranged as a three-dimensional network.

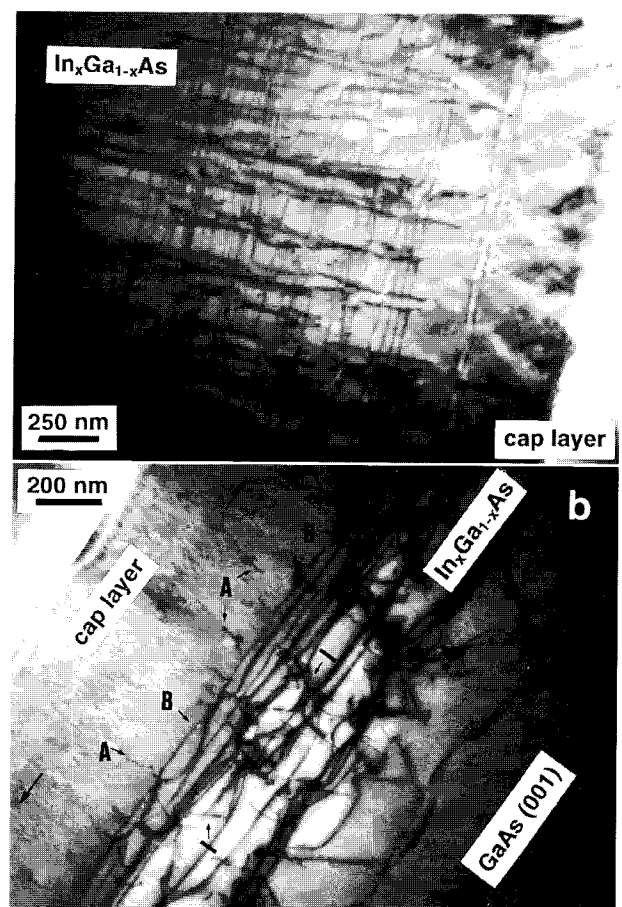
Threading segments between two misfit segments are visible in the graded layer in XTEM and PVTEM micrographs. In PVTEM images, such segments are easily identified by a characteristic 'zig-zag' contrast (see dislocations marked as 'T' in Fig. 2b and 4b) while in XTEM images, these segments are not parallel to the growth interface (001) ('I' in Fig. 2b).

Table 1 shows the In content and the strain relaxation of each cap layer, determined from DCXRD measurements, as well as the thicknesses of the cap layers measured by XTEM.

The arrays of misfit dislocations are asymmetrically distributed for the two mentioned $\langle 110 \rangle$ directions and this is probably owing to the basic asymmetry of the orthogonal edge and 60° dislocations in the zinc blende structure (α or β character).¹⁴ Peierls barriers between two types of dislocations lead to unequal mobilities for the arrays of dislocations along the $\langle 110 \rangle$ directions. Dislocation density data in Fig. 3 for the specimen A graded layer support this assumption. This fact is clearly observed in Fig. 2b where dislocations labelled as A, running parallel to the electron beam, reach higher than

Table 2 Experimental TEM and theoretical results obtained for graded layers in nanometres; h is graded layer total thickness, z_c^1 and z_c^2 are two critical thicknesses measured in both $\langle 110 \rangle$ directions as shown in Fig. 3; z_c^1 and z_c^2 correspond to predicted critical thicknesses using Tersoff and Dunstan models, respectively

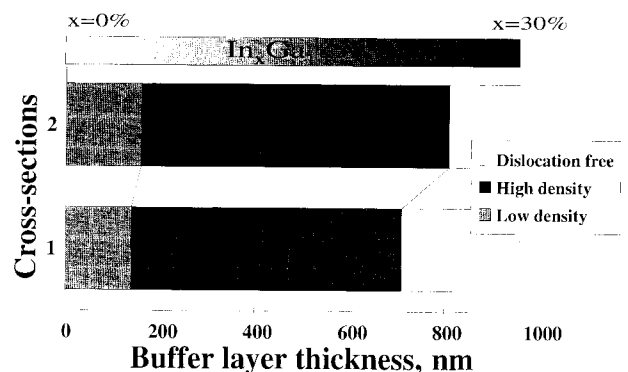
Specimen	h	z_c^1	z_c^2	z_c^1	z_c^2
A	...	710	810	817 ± 4	684
B	950	660	650
C	...	740	790



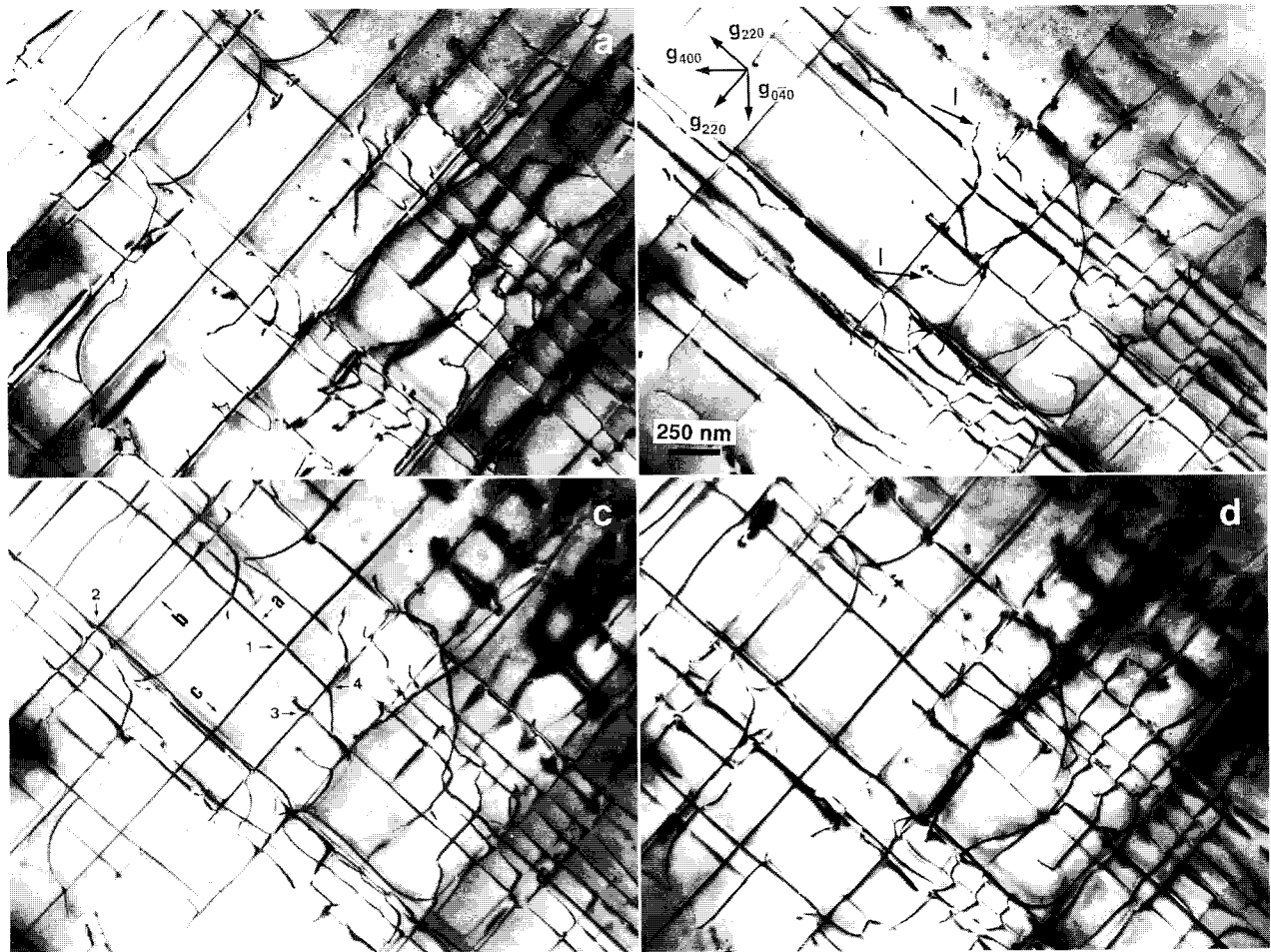
2 a Plan-view TEM micrograph (bright field (BF) $g = (220)$) showing dislocation network, b cross-sectional TEM micrograph (BF $g = (220)$) showing dislocation distribution

those lying perpendicular (B). Thus, the critical thickness z_c is different for the two $\langle 110 \rangle$ directions.

A representative example of the observed misfit dislocations is shown in the micrographs of Fig. 4 for the diffraction vectors $g_{(220)}$, $g_{(400)}$ and $g_{(040)}$. A characteristic contrast is seen near 'a' in Fig. 4c where a dislocation parallel to $[110]$ becomes invisible for g_{220} reflection. Applying the conventional invisibility criterion $g \cdot b = 0$, this dislocation appears to be of pure edge type with $b = \frac{1}{2}[110]$. Following a similar procedure, the dislocations labelled as 'b' and 'c' are also of pure edge type with $b = \frac{1}{2}[110]$. These edge dislocations with b parallel to the



3 Schematic representation of dislocation density distribution in InGaAs buffer layer of specimen A: dislocation density is below $5 \times 10^8 \text{ cm}^{-2}$ for low dislocation density region and $8.7 \pm 1 \times 10^9 \text{ cm}^{-2}$ for dislocation rich area



a g_{220} ; b g_{220} ; c g_{400} ; d g_{040} reflections

4 Plan-view TEM micrographs showing dislocation network in grading layer

(001) growth plane are expected since they provide the most efficient strain relief. Many of the dislocations in the figure are 60° dislocations. These dislocations were the most frequent in this system. From the invisibility criteria and statistical observations, a $30 \pm 8\%$ of edge dislocations is estimated. These are mainly concentrated near the graded layer/substrate interface.

In these micrographs (Fig. 4) several dislocation interactions are observed. The most frequent interactions are typical reactions between 60° dislocations, as can be seen at the lower right corners of the micrographs of Fig. 4. On the other hand, numerous dislocations crossing without any interaction appear in the PVTEM images shown in Fig. 4. This can be attributed to one of the following configurations: (a) two 60° dislocations with perpendicular Burgers vectors, (b) two pure edge dislocations (point 1 in Fig. 3c), and (c) dislocations contained in different planes (001), that is the most probable configuration in this system (point 2 in Fig. 3c).

Single and multiple dislocation loops, without any fixed pattern, are found by XTEM deep into the graded layer, in some cases reaching the substrate (Fig. 5). The deepest observed loop penetrates about $1 \mu\text{m}$ into the substrate.

A Burgers vector analysis of the dislocations in these kinds of loops is shown in Fig. 6a–d using g_{111} , g_{111} , g_{220} , and g_{004} two-beam conditions respectively. For the g_{220} condition three loops are visible. For the g_{111} reflection a considerable reduction of contrast occurs for the dislocation labelled as 1, which is consistent with 60° dislocations with $b = \frac{1}{2}[011]$ or $\frac{1}{2}[101]$. The smallest loop 2 becomes invisible for the g_{111} reflection and therefore it is a 60° dislocation

with $b = \frac{1}{2}[0\bar{1}1]$ or $\frac{1}{2}[\bar{1}01]$. Dislocation 3 is clearly of edge type with $b = \frac{1}{2}[\bar{1}10]$ because of the invisibility for the g_{004} reflection.

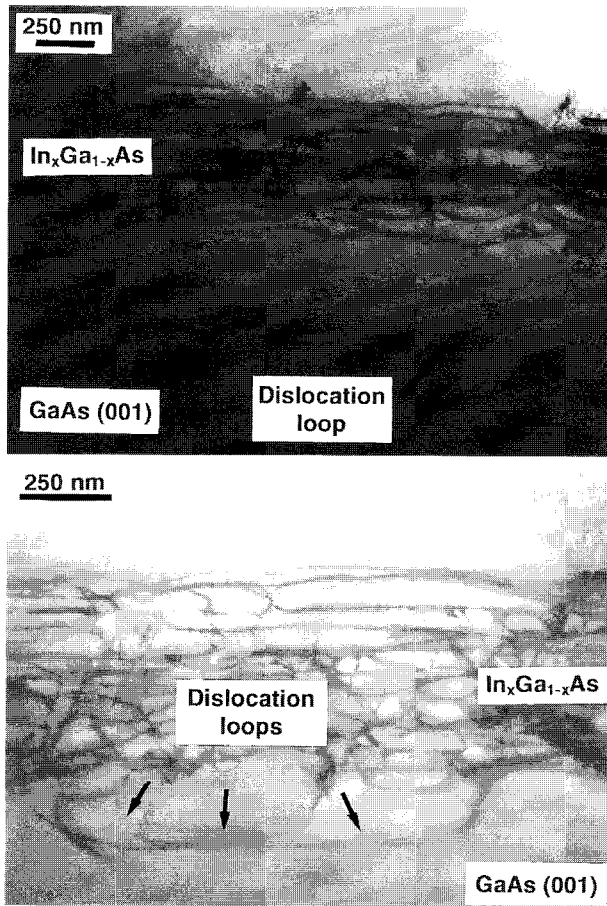
Dislocation loops penetrating deep into the substrate in graded structures were previously reported by Le Goues *et al.*¹⁵ All the loops were observed to have identical Burgers vectors, which is a typical result of the dislocation multiplication Frank–Read mechanism. In that paper,¹⁵ the authors proposed a mechanism of loop multiplication where a single pinned dislocation segment acts as a Frank–Read centre. However, in the present study, dislocation loops with different Burgers vectors are observed to penetrate into the substrate. Therefore, the Le Goues *et al.* interpretation of their existence in the substrate can not be applied here.

Theoretical models

In recent years, two authors have proposed models to predict the existence of a strained region free of dislocations at the top of a linearly graded composition layer. The first model is based on geometrical considerations¹⁶ and the second is an energy based model.⁷ These models are briefly commented upon and applied to this system in the following paragraphs.

TERSOFF'S MODEL

Recently, Tersoff⁷ deduced the equilibrium dislocation distribution and the residual strain in linearly graded



a deep inside substrate; b without penetrating into substrate

5 Cross-sectional TEM images (BF $g = (2\bar{2}0)$) showing dislocation loops

composition layers. The density of dislocations in equilibrium (it is assumed that the energetic formation of dislocations is balanced by the elastic energy of the structure assuming that the dislocations adapt the lattice parameter perfectly up to an equilibrium thickness z_c) is calculated assuming a film thickness much larger than the dislocation spacing. No dislocation interaction is considered.

Such considerations permit the calculation of the parameter z_c for a linearly graded composition layer

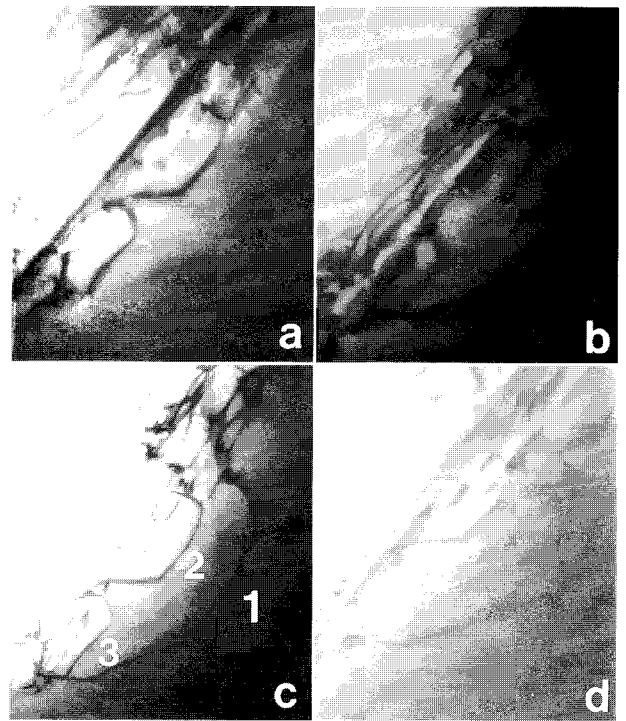
$$z_c = h - \left(\frac{E_d}{b_{90^\circ} \cdot \mu \cdot \epsilon'} \right)^{1/2} \dots \dots \dots (1)$$

where E_d is the energy of the dislocation per unit length, h the total thickness of the grading layer, b_{90° the misfit component of the Burgers vector of the dislocation, $\epsilon' = d\epsilon(z)/dz$, $\epsilon(z)$ being the mismatch strain, and μ the elastic shear modulus ($3.09 \times 10^8 \text{ N m}^{-2}$).

For the system considered here, assuming an isotropic medium, E_d is calculated as follows¹⁷

$$E_d = \frac{\mu b^2}{4\pi} \left[\cos^2 \beta + \frac{\sin^2 \beta}{1-\nu} \right] \ln \frac{\alpha R}{b} \dots \dots \dots (2)$$

where β is the angle between the Burgers vector and the dislocation line, α the dislocation core corrector parameter, R the cut off parameter and ν the Poisson's ratio of the film (0.33). Parameter α has been usually taken as 3 or 4 for calculations involving semiconductor materials, although the value $\alpha = 1$ is now more often used. However, in the present work the value $\alpha = 2.45$ is used as this is the value measured for InGaAs.¹⁸



a g_{111} ; b g_{111} ; c g_{220} ; d g_{004}

6 XTEM images showing three dislocation loops for different reflections

If 60° dislocations and $R = 50 \text{ nm}$ are assumed and Vegard's law is assumed, $z_c = 801 \text{ nm}$ is deduced. Taking into account the experimental percentage of each type of dislocation: $30 \pm 8\%$ of pure edge dislocations, z_c is $817 \pm 4 \text{ nm}$. In this calculation both b and μ are taken as the average values corresponding to a 15%In content.

In this model, changes in α or R parameters slightly affect the resulting value of z_c but, on increasing the proportion of edge type versus 60° type dislocations, while the total dislocation density remains constant, the final z_c value varies less than 4.5%: z_c ($\alpha = 2.45$, $R = 50 \text{ nm}$, $h = 1000 \text{ nm}$, 100% of 60°) = 847 nm and z_c ($\alpha = 2.45$, $R = 50 \text{ nm}$, $h = 1000 \text{ nm}$, 100% of edge) = 887 nm.

This model allows us to calculate the dislocation density in the graded layer from the expression

$$\rho = \frac{\epsilon'}{b} \dots \dots \dots (3)$$

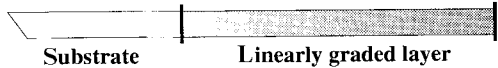
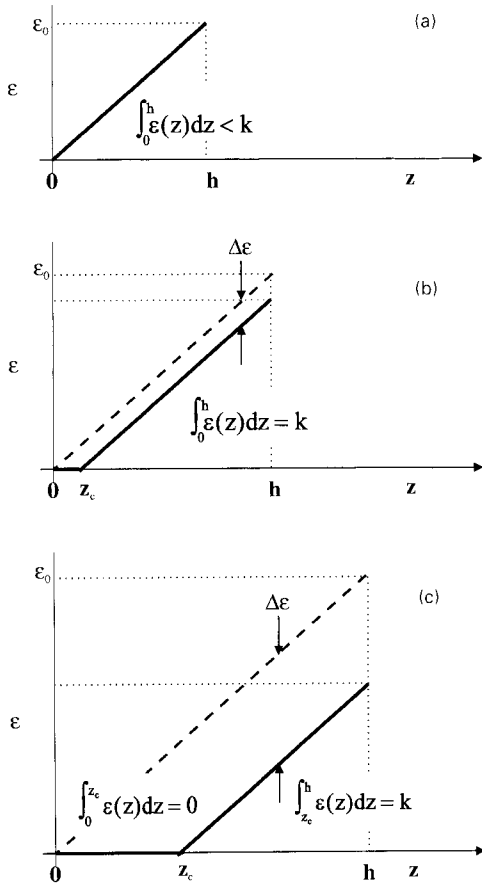
and considering 100% of 60° dislocations, the theoretical ρ is $11.2 \times 10^9 \text{ cm}^{-2}$. If we consider 22 or 38% of pure-edge dislocations ρ is 9.4 or $8.5 \times 10^9 \text{ cm}^{-2}$, respectively. Notice that the experimental density measured by TEM falls between these two values.

DUNSTAN'S MODEL

Dunstan *et al.*⁸ proposed a model based solely on geometrical considerations. The obtained expression does not explicitly consider either strain energies or dislocation energies. It is based on simple arguments that can be summarised as follows: (a) at small thicknesses, the layer does not relax because the relaxation energy $\Delta\epsilon = b/md$ exceeds the strain ϵ in the layer. (b) the layer may begin to relax when the condition $b md = \epsilon$ is reached (where m is a factor between 1 and 2). Thus, this model predicts that the strain-thickness product of a single layer must be a constant

$$h\epsilon = k \dots \dots \dots (4)$$

where k is 0.8 nm for the InGaAs/GaAs system, ϵ is the strain and h the total thickness of the epilayer. As recently



a before reaching condition $\int_0^h \epsilon(z) dz = k$ no dislocations relax the layer; b when this condition is attained, dislocations located between 0 and z_c relax totally this region; c following growth, more dislocations relax the first region (i.e. $\int_0^{z_c} \epsilon(z) dz = 0$) so that a defect free region following $\int_{z_c}^h \epsilon(z) dz = k$ always stays at top of grading

7 Schematic description of strain relaxation Dunstan mechanism during growth of linearly graded layers

published,¹⁹ this expression also describes the strain relaxation in more complex structures (stacks of layers, graded layers, etc.) considering the average strain and the total thickness.

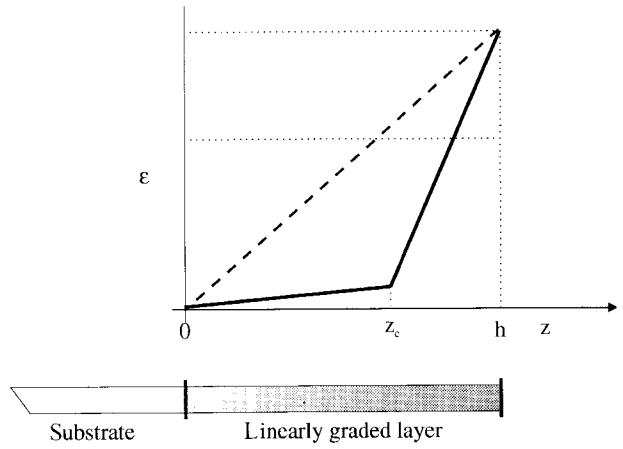
For a linearly graded layer, the average strain is

$$\bar{\epsilon} = \frac{\int_0^h \epsilon(z) dz}{\int_0^h dz} = \epsilon' \frac{z}{2} \dots \dots \dots (5)$$

where ϵ' is the misfit strain rate $d\epsilon/dz$.

This induces a strain relaxation behaviour schematically described in Fig. 7. When $\int \epsilon(z) dz$ is less than k the relaxation does not start (Fig. 7a), but when this value is reached, dislocations relax the layer between 0 and z_c so that no strain remains in this region. When growing graded structures, a strained and defect free region always remains at the top of the grading with the thickness $h-z_c$ that depends only on the grading rate ϵ' (Fig. 7b and c). As shown in Fig. 7, the thickness of this strained top region is determined by the condition

$$\int_{z_c}^h \epsilon(z) dz = k = 0.8 \text{ nm} \dots \dots \dots (6)$$



8 Schematic description of real relaxation occurring in linearly graded layers: as no total relaxation is possible, area below curve between 0 and z_c is no longer 0 and therefore z_c becomes higher to reduce area between z_c and h

as from equation (4)

$$h\bar{\epsilon} = \int_0^h dz \frac{\int_0^h \epsilon(z) dz}{\int_0^h dz} = \int_0^{z_c} \epsilon(z) dz + \int_{z_c}^h \epsilon(z) dz = \int_{z_c}^h \epsilon(z) dz = k \dots \dots \dots (7)$$

The predicted z_c is 684 nm. In this model, the z_c value only depends on the graded layer total thickness and on the grading rate.

COMPARISON BETWEEN THE THEORETICAL MODELS AND THE EXPERIMENTAL RESULTS

The model that more closely follows the experimental results is the Dunstan model. Surprisingly, a lower z_c value than the experimental one is predicted. To understand this difference, it is necessary to note that in all the existing models, a step by step total relaxation is assumed to occur during the growth. Obviously, this can never happen. A convincing argument is that a single layer can not relax more than 70%.²⁰ Because of this, the dislocation-rich region needs to be larger to reach the same lattice parameter and the first term of the Dunstan condition becomes $\int_0^{z_c} \epsilon(z) dz \neq 0$

$$\bar{\epsilon} h = \int_0^{z_c} \epsilon(z) dz + \int_{z_c}^h \epsilon(z) dz \dots \dots \dots (8)$$

and, as is shown in Fig. 8, z_c needs to be higher, as the area below the curve remains constant.

Conclusion

A detailed study of the dislocation behaviour in compositionally graded InGaAs buffer layers on GaAs substrate is presented. Dislocations adapting the lattice parameter up to a thickness z_c are observed. A top dislocation free region ($< 10^5 \text{ cm}^{-2}$) is evident. In addition to this very promising result it must be noted that dislocation loops penetrating deep into the substrate are also evident. A simple force balance model is presented to interpret this dislocation behaviour. Comparison of the experimental data with several existing models shows that the geometrical Dunstan

model agrees more closely with the experimental results. Moreover, some explanations for the differences observed between the experimental observations and the model predictions are given. The most important and practical outcome is that once the relaxation process is understood, the strain relaxation control in such linearly graded structures will allow the growth of very efficient buffer layers for InGaAs based devices on GaAs substrates.

Acknowledgements

The authors would like to thank Guillermo Aragón for fruitful discussions. The present work has received support from the Comisión Interministerial de Ciencia y Tecnología (CICYT) (MEC), BLES Proyect (Esprit Program, ref. no. 6854) and Junta de Andalucía, under group no. 6020. This study was carried out at the División de Microscopía Electrónica de la Universidad de Cádiz.

References

1. F. K. LE GOUES, B. S. MEYERSON, J. F. MORAR, and P. D. KIRCHNER: *J. Appl. Phys.*, 1992, **71**, 4230–4243.
2. J. C. P. CHANG, T. P. CHIN, C. W. TU, and K. L. KAVANAGH: *Appl. Phys. Lett.*, 1993, **63**, 500–502.
3. J. C. P. CHANG, J. CHEN, J. M. FERNÁNDEZ, H. H. WIEDER, and K. L. KAVANAGH: *Appl. Phys. Lett.*, 1992, **60**, 1129–1131.
4. V. KRISHNAMOORTHY, Y. W. LIN, and R. M. PARK: *J. Appl. Phys.*, 1992, **72**, 1752–1757.
5. S. M. LORD, B. PEZISHKI, S. D. KIM, and J. S. HARRIS: *J. Cryst. Growth*, 1993, **127**, 759–764.
6. A. FISCHER-COLBRIE, R. D. JACOWITZ, and D. G. AST: *J. Cryst. Growth*, 1993, **127**, 560–565.
7. J. TERSOFF: *Appl. Phys. Lett.*, 1993, **62**, 693–695.
8. D. J. DUNSTAN, S. YOUNG, and R. H. DIXON: *J. Appl. Phys.*, 1991, **70**, 3038–3045.
9. J. HORNSTRA and W. J. BARTELS: *J. Cryst. Growth*, 1978, **44**, 513–517.
10. M. A. G. HALLIWELL: 'Advances in X-ray analysis', (ed. C. S. Barrett), 33–61; 1990, New York, Plenum Press.
11. L. K. HOWARD, P. KIDD, and R. H. DIXON: *J. Cryst. Growth*, 1992, **125**, 281–290.
12. P. KIDD, P. F. FEWSTER, N. L. ANDREW, and D. J. DUNSTAN: *Inst. Phys. Conf. Ser.*, 1993, **134**, 585–589.
13. P. KIDD and R. H. DIXON: *Inst. Phys. Conf. Ser.*, 1991, **117**, 661–665.
14. B. A. FOX and W. A. JESSER: *J. Appl. Phys.*, 1990, **68**, 2739–2746.
15. F. K. LE GOUES, B. S. MEYERSON, and J. F. MORAR: *Phys. Rev. Lett.*, 1991, **66**, 2903–2906.
16. A. SACEDÓN, F. GONZÁLEZ-SANZ, E. CALLEJA, E. MUÑOZ, S. I. MOLINA, F. J. PACHECO, D. ARAÚJO, R. GARCÍA, M. LOURENÇO, Z. YANG, P. KIDD, and D. DUNSTAN: submitted to *Appl. Phys. Lett.*
17. J. P. HIRSCH and J. LOTHE: 'Theory of dislocations', 2nd edn; 1982, New York, Wiley-Interscience.
18. S. I. MOLINA: PhD thesis, Universidad de Cádiz, Spain, 1993.
19. D. J. DUNSTAN, P. KIDD, P. F. FEWSTER, N. L. ANDREW, R. GREY, J. P. R. DAVID, L. GONZÁLEZ, Y. GONZÁLEZ, A. SACEDÓN, and F. GONZÁLEZ-SANZ: *Appl. Phys. Lett.*, 1994, **65**, 839–842.
20. V. KRISHNAMOORTHY, Y. W. LIN, L. CALHOUN, H. L. LIU, and R. M. PARK: *Appl. Phys. Lett.*, 1992, **61**, 2680–2683.

SURFACE MODIFICATION TECHNOLOGIES CD-ROM

Full text and illustrations from SMT VII, VIII, IX, X and XI. Search by subject category or use full text search. Requires IBM-compatible PC with 486 or higher, 1MByte hard disk space, 256 colour SVGA display with 1024 x 768 resolution, windows 3.1 or higher. Rapid response and simple installation.

PD 700

European Union £200/Members £160 Non-European Union \$300/Members \$240
p&p European Union £5.00/Non-EU \$10.00

Orders to: The Accounts Department, IOM Communications Ltd, 1 Carlton House Terrace,
London SW1Y 5DB Tel: +44 (0) 171 451 7300 Fax: +44 (0) 171 839 4534
Email: Marketing@materials.org.uk Internet: www.instmat.co.uk



IOM Communications

IOM Communications Ltd is a wholly-owned subsidiary of The Institute of Materials.